

---

Doctoral Dissertations

Student Theses and Dissertations

---

1972

## Grain boundary diffusion in ionic crystals

Kulwant Singh Sabharwal

Follow this and additional works at: [https://scholarsmine.mst.edu/doctoral\\_dissertations](https://scholarsmine.mst.edu/doctoral_dissertations)



Part of the [Metallurgy Commons](#)

Department: **Materials Science and Engineering**

---

### Recommended Citation

Sabharwal, Kulwant Singh, "Grain boundary diffusion in ionic crystals" (1972). *Doctoral Dissertations*. 204.  
[https://scholarsmine.mst.edu/doctoral\\_dissertations/204](https://scholarsmine.mst.edu/doctoral_dissertations/204)

This thesis is brought to you by Scholars' Mine, a service of the Missouri S&T Library and Learning Resources. This work is protected by U. S. Copyright Law. Unauthorized use including reproduction for redistribution requires the permission of the copyright holder. For more information, please contact [scholarsmine@mst.edu](mailto:scholarsmine@mst.edu).

GRAIN BOUNDARY DIFFUSION

IN IONIC CRYSTALS

by

KULWANT SINGH SABHARWAL, 1944-

A DISSERTATION

Presented to the Faculty of the Graduate School of the

UNIVERSITY OF MISSOURI - ROLLA

In Partial Fulfillment of the Requirements for the Degree

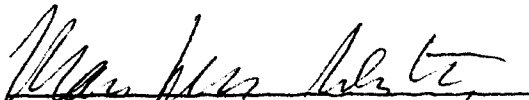
DOCTOR OF PHILOSOPHY


in

METALLURGICAL ENGINEERING

1972

T2771  
86 pages  
c.1

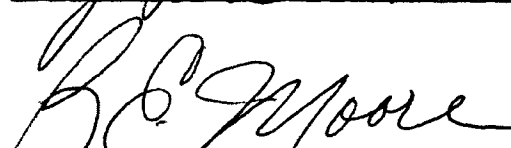
  
\_\_\_\_\_  
Advisor

  
\_\_\_\_\_

  
\_\_\_\_\_

  
\_\_\_\_\_

\_\_\_\_\_  
\_\_\_\_\_

  
\_\_\_\_\_

## ABSTRACT

The diffusion of  $^{131}\text{I}$  in single crystals and along the tilt grain boundaries of pure and calcium chloride doped ( $142 \pm 5$  ppm) bicrystals of sodium chloride, grown by Czochralski technique, was investigated using a microtome sectioning technique. Results on bulk diffusion in pure NaCl agree well with the results of earlier investigators and are represented by

$$D = (504 \text{ cm}^2/\text{sec}) \exp(-2.27 \text{ eV}/kT).$$

Enhanced diffusion of  $^{131}\text{I}$  is observed along the grain boundaries and the presence of the dopant lowers the grain boundary diffusivity over the entire temperature range of  $430^\circ\text{C} - 570^\circ\text{C}$  studied in the present investigation. Thermal activation and electrical polarization effects, acting simultaneously on the diffusing ion, determine the magnitude of the grain boundary diffusivity in these ionic bicrystals. In the low temperature range of  $430^\circ\text{C} - 490^\circ\text{C}$ , the diffusion of  $^{131}\text{I}$  along the grain boundaries is described by the relationship

$$D'\delta = (D'\delta)_0 \exp(-Q_b/kT),$$

where  $(D'\delta)_0$  has values of  $8.45 \times 10^{-5}$  and  $0.39 \text{ cm}^3/\text{sec}$

for the pure and the doped bicrystals, respectively.  $Q_b$  is observed to be 1.36 and 1.93 eV for the same two cases. In the high temperature range of 490°C - 570°C, grain boundary charge and ionic polarization cause distinct but similar diffusion anomalies in the grain boundary diffusivity plots of both the pure and the doped bicrystals, depending upon the proximity of the measuring temperature to the isoelectric temperature. Grain boundary diffusion seems to occur by movement of ions in the grain boundary core by an "interstitial" motion of iodine ions.

## ACKNOWLEDGMENTS

The author wishes to express his sincere appreciation to Professor Manfred Wuttig for suggesting this problem and for his encouragement and advice throughout the course of this work.

The author also wishes to thank Dr. Harry Weart, Chairman of the Metallurgy Department, for his able guidance in absence of the author's advisor.

Financial assistance by the Department of Metallurgical Engineering during four years of graduate work is greatly appreciated.

This work was supported by the Advanced Research Project Agency of the Department of Defense.

## TABLE OF CONTENTS

	PAGE
ABSTRACT . . . . .	ii
ACKNOWLEDGMENT . . . . .	iv
LIST OF ILLUSTRATIONS . . . . .	vi
LIST OF TABLES . . . . .	vii
I. INTRODUCTION . . . . .	1
II. REVIEW OF LITERATURE . . . . .	3
A. SINGLE CRYSTAL DIFFUSION . . . . .	3
B. GRAIN BOUNDARY DIFFUSION . . . . .	5
III. THEORY . . . . .	10
A. GRAIN BOUNDARY CHARGE . . . . .	10
B. BULK DIFFUSION COEFFICIENT . . . . .	15
C. GRAIN BOUNDARY DIFFUSION COEFFICIENT . . . . .	17
IV. EXPERIMENTAL PROCEDURES . . . . .	20
A. CRYSTAL GROWING . . . . .	20
B. SAMPLE PREPARATION, SECTIONING, COUNTING AND AUTORADIOGRAPHY . . . . .	25
C. EXPERIMENTAL DATA AND ESTIMATION OF ERRORS . . . . .	28
V. EXPERIMENTAL RESULTS . . . . .	42
A. SINGLE CRYSTAL DIFFUSION COEFFICIENTS . . . . .	42
B. GRAIN BOUNDARY DIFFUSION COEFFICIENTS . . . . .	45
VI. DISCUSSION . . . . .	53
VII. CONCLUSIONS . . . . .	73
BIBLIOGRAPHY . . . . .	74
VITA . . . . .	79

## LIST OF ILLUSTRATIONS

FIGURE	PAGE
1. $^{131}\text{I}$ Iodine Penetration Profile of A "Pure" Bicrystal Sample Showing the Bulk and Grain Boundary Diffusion . . . . .	30
2. A Typical Series of Autoradiographs of the Bicrystal Diffusion Sample of Figure 1 Taken During Sectioning at Various Penetration Depths . . . . .	32
3. A Typical $^{131}\text{I}$ Iodine Penetration Profile of a Single Crystal Sample . . . . .	35
4. A Typical $^{131}\text{I}$ Iodine Penetration Profile of a $\text{CaCl}_2$ Doped ( $142\pm 5$ ppm) Bicrystal Sample . . . . .	38
5. Arrhenius Plots of $^{131}\text{I}$ Iodine Single Crystal Diffusion Coefficients for "Pure" and $\text{CaCl}_2$ Doped Sodium Chloride . . . . .	44
6. Plots Showing the Variation of the $^{131}\text{I}$ Iodine Grain Boundary Diffusion Parameter, $D'\delta$ , with Temperature for "Pure" and $\text{CaCl}_2$ Doped ( $142\pm 5$ ppm) Sodium Chloride Bicrystal Samples . . . . .	48
7. A Schematic Sketch of the $\ln D'\delta$ vs $1/T$ Plots Shown in Figure 6 . . . . .	50
8. Sketch Showing Variation of $e\phi$ with Distance $x$ from the Grain Boundary Core into the Bulk for Temperatures Other than the Isoelectric Temperature in Ionic Crystals . . . . .	63

## LIST OF TABLES

TABLE	PAGE
I. TYPICAL ANALYSIS OF HARSHAW SODIUM CHLORIDE . .	21
II. ANALYSIS OF SODIUM CHLORIDE BICRYSTAL DOPED WITH CALCIUM CHLORIDE . . . . .	24
III. ACTIVATION ENERGIES AND PRE-EXPONENTIAL FACTORS OF IODINE GRAIN BOUNDARY DIFFUSION . .	51
IV. ENTHALPIES AND ENTROPIES OF FORMATION AND MOTION OF VARIOUS DEFECTS IN SODIUM CHLORIDE .	54



## I. INTRODUCTION

In any real crystalline solid, imperfections such as dislocations, free surfaces and grain boundaries exist, and the mean jump frequency of an atom in these regions tends to be much higher than that of an atom in the lattice. The diffusivity therefore tends to be higher in these regions and this has been well established in the case of metals. In ionic crystals, however, there have been conflicting reports about enhancement of cation and anion diffusivities at the grain boundaries. The difficulty in the grain boundary diffusivity studies in ionic crystals like NaCl arises because the dislocations and grain boundaries in these crystals are associated with an electrical dipole layer. Since the movement of the ions occurs by means of electrically charged point defects, their interaction with the long range electrical fields arising from these line and surface defects can conceivably have a strong effect upon the dislocation and grain boundary diffusion.

Earlier work on  $^{36}\text{Cl}$  and  $^{22}\text{Na}$  grain boundary diffusion in NaCl was done by Riggs<sup>1</sup> using the same technique of microtome sectioning which is employed in the present study. He showed an Arrhenius-type plot for anion grain boundary diffusivity in the temperature range of 420°C - 480°C. This temperature range is below

the isoelectric temperature of NaCl. As Riggs did not explore grain boundary diffusivity behavior over a wide enough temperature range, his study was inconclusive with regard to the effect of an electrical dipole layer on grain boundary diffusivity. It was therefore the purpose of the present work to extend the temperature range of anion grain boundary diffusivity study such that the effect of the charge on diffusivity could be established, and to determine, if possible, the effect of divalent cation dopant on grain boundary diffusion. The isotope  $^{131}\text{I}$  was chosen for the present study instead of  $^{36}\text{Cl}$  in order to reduce the experimental errors in counting due to the background activity, as  $^{131}\text{I}$  is available in much higher specific activities than  $^{36}\text{Cl}$ . Iodine ion was also preferred over chlorine ion because, if there were to be any observable effect of the electrical dipole layer on anion grain boundary diffusivity, it was expected to be more evident with iodine ion as it is more polarizable than chlorine ion.

## II. REVIEW OF LITERATURE

### A. Single Crystal Diffusion

A large number of investigators have studied self-diffusion of ions in monocrystalline alkali halides at high temperature (above  $0.7 T_m$ ) using both the conventional sectioning<sup>2-5</sup> and isotropic exchange techniques.<sup>6-8</sup> Fortunately, the available experimental results present an extremely coherent picture of the high temperature diffusion mechanism which is a single-vacancy mechanism for both the anions and cations. At high temperatures, the displacement of ions is attributed to the presence of Schottky defects, the validity of the Einstein relation and the values of activation energies being the strongest arguments in favor of this interpretation.

At low temperatures, the number of thermal defects becomes small and the properties of ionic crystals are explained by the presence of defects more complex than Schottky defects. The explanation of the diffusion behavior of cations differs from that of anions in this temperature range. Diffusivity and conductivity measurements in NaCl by different investigators<sup>3,9</sup> indicate the existence of a low temperature region where the activation energy of cation self-diffusion is observed to be lower than at higher temperatures. This effect on the mobility of the cations is tied to the

presence of impurities. The dissolved aliovalent impurities in NaCl (most frequently divalent) locate substitutionally on the sodium lattice site, thereby increasing the number of sodium vacancies. These excess sodium vacancies introduced with the cation impurities contribute to the reported increased cation diffusivity at low temperatures. The failure of the Einstein relation at low temperatures is also explained by the association of the excess cation vacancies with the divalent cation impurities; the complexes thus formed are neutral and do not contribute to the conductivity whereas the whole of the vacancies, associated and non-associated, take part in diffusion.

It is difficult to increase the concentration of anionic vacancies in a like manner by adding multivalent anions which are in general not very stable in alkali halides.<sup>5</sup> The presence of divalent cation impurities lowers the concentration of the anion vacancies due to the law of mass action.<sup>10</sup> If the anion diffusion in NaCl were to occur by single-vacancy mechanism alone, the chlorine self-diffusivity should exhibit high and low temperature ranges with the transition occurring at the same temperature as that of the "knee" in the cation diffusivity plot. However, the experimental observations of different investigators do not support this view. The results of Laurance<sup>5</sup> and others<sup>11,12</sup> indicate that the

diffusion of anions such as chlorine in NaCl takes place both by a single-vacancy mechanism and by a vacancy pair mechanism, the latter process being preponderant at low temperatures and in the presence of divalent cation concentrations exceeding 100 ppm.<sup>5</sup>

Some investigators have also studied diffusion of foreign ions in the alkali halides. Chemla<sup>2</sup> studied diffusion of  $I^-$ ,  $Br^-$  and  $Cl^-$  in NaCl and Beaumont and Cabane<sup>13</sup> that of  $I^-$  in NaCl and KCl. Beaumont and Cabane found the activation energies of  $Cl^-$  and  $I^-$  in NaCl to be the same while in Chemla's work they were of the same order of magnitude. A single-vacancy mechanism has been shown to be most likely in such heterodiffusion studies.

#### B. Grain Boundary Diffusion

Laurant and Benard's work<sup>14</sup> was probably the first systematic attempt to study the diffusion phenomenon in sintered polycrystalline alkali halide samples. Their early work indicated that the activation energy for the diffusion of anions along the grain boundaries was essentially the same as the activation energy for anion single crystal diffusion. They further observed that the self-diffusion coefficients of the anions are increased by the presence of grain boundaries and that the migration rate of anions increases as the mean

dimensions of the crystal comprising the polycrystalline aggregate become smaller. They said that it is possible to connect this increase in speed of anion diffusion with polarization of the ions. On the basis of their results of grain boundary diffusivity in different halides of potassium, they showed (Fig. 5 of their paper) that the increase in grain boundary diffusivity of different anions is directly proportional to the polarizability of the anions. Thus they concluded that any tentative attempt at theoretical explanation of the grain boundary diffusivity phenomenon would have to take, as a base, the properties of the polarization of the ions.

Cabane's work<sup>15</sup> on polycrystalline KI subsequently showed that by improving the quality of the samples by exclusion of moist atmosphere during sintering and annealing, the activation energy of anion grain boundary diffusion was observed to be about half that in single crystalline material. His work on different anions also confirmed Laurant and Benard's relation between polarization of ions and their diffusion at the grain boundaries. The results of Riggs<sup>1</sup> also indicate an increase in  $\text{Cl}^-$  diffusion coefficient along the grain boundaries of pure and  $\text{CaCl}_2$  doped bicrystals and a decrease in the activation energy in a manner similar to that of Cabane.

Riggs further observed that the grain boundary angle, the grain boundary character (tilt or twist) and the divalent cation concentration had no significant effect on the anion diffusion rates. The ionic movement was believed to occur in the grain boundary core region and to consist of the movement of "interstitial" type chlorine ions. This "interstitial" type mechanism was proposed on the basis of the measured activation energy values. Activation energy of  $^{36}\text{Cl}$  diffusion in NaCl bicrystals was observed to be almost half of the activation energy needed for single-vacancy mechanism and an even smaller fraction of the value for vacancy pair mechanism. Since activation energies for interstitial type mechanism in metals are observed to have such small magnitudes, an "interstitial" type mechanism was thought to be operative along the comparatively open core regions of grain boundaries in NaCl.

In contrast to the results of anion diffusion, the weight of the experimental evidence<sup>1,14-17</sup> on cation diffusion in alkali halides shows that enhanced cation diffusion is not observed in the grain boundaries.

It has always been difficult to interpret the diffusivity data in high-angle grain boundaries because the exact structure of these boundaries is not completely known. Although a large number of models have been proposed by different investigators,<sup>18-23</sup> none of them

is fully satisfactory for the high-angle grain boundaries. Only the structure of small-angle grain boundaries in solids is well understood and is said to consist of stable arrays of dislocations.<sup>24</sup> It can be argued that the interactions between dislocations in the high-angle grain boundaries should tend to destroy their directionality. However, there have been a number of investigations<sup>25-27</sup> which indicate that high-angle grain boundaries are not isotropic and that even at maximum misorientation angles, they retain some characteristics of a dislocation structure. In a dislocation core or in any hard sphere model of a grain boundary, there are many relatively open regions. In these regions, the energy to form a vacancy or move an atom into a vacancy will be lower than in the lattice and hence, qualitatively, the values of activation energy for self-diffusion in the grain boundaries are observed to be smaller than in the bulk. However, no quantitative treatment has been given in the literature to explain the enhanced diffusion observed in the high-angle grain boundaries.

During the last three decades, many investigators<sup>28-33</sup> have done a considerable amount of work on the theory of charged defects, with particular emphasis on alkali halide crystals. According to this theory, an electrical dipole layer develops around dislocations,



external surfaces and grain boundaries of ionic crystals. The electrical fields developed due to the dipole layer could possibly have a strong effect on the movement of a diffusing ion in alkali halides. Most of the research in the past has been on the development of this theory and on experimental investigation of the sign of the charge<sup>34-36</sup> carried by the dislocations in these crystals. It has now been well established that the edge dislocations are positively charged above the isoelectric temperature of the material while they carry a negative charge below this temperature. Screw dislocations remain uncharged at all temperatures.<sup>35,36</sup> Research work on establishing a relationship between the electrical dipole layer and the grain boundary diffusivity in ionic crystals seems to be lacking in the literature.

### III. THEORY

#### A. Grain Boundary Charge

The existence of an electrical dipole layer around the surfaces of ionic crystals, in which Schottky defects predominate, was first proposed by Frenkel<sup>28</sup> in 1946. Since then, a number of investigators<sup>29-33</sup> have developed this idea into a theory of charged defects, applicable under varied conditions in ionic crystals. Qualitatively the surface dipole region arises in the following manner. In materials like NaCl, the free energy necessary to form a cation vacancy is less than that required to form an anion vacancy. Hence when the temperature is raised from absolute zero, an excess of cation vacancies is emitted from the surface into the crystal, leaving a net positive charge on the surface and a region of negative space charge beneath the surface. The resulting space charge distribution increases the energy of formation of cation vacancies in the interior of the crystal by the energy necessary to move them across the dipole layer. The energy of formation of anion vacancies in the bulk is reduced in the same manner. The result is that, in equilibrium, there will exist a dipole region at the surface across which there exists a potential difference which serves

to adjust the free energies of vacancies in such a way that the bulk of the crystal remains electrically neutral.

The edge dislocations, being sources and sinks for vacancies, behave in many respects like a surface. One can therefore expect<sup>37</sup> the edge dislocations in an ionic crystal to be charged and to be surrounded by a sheath of vacancies of predominately the opposite sign. Clearly, a grain boundary or a mosaic boundary should also be charged and surrounded by a balancing layer of charge, whether one regards the boundary as essentially a junction between two separate blocks of crystal or as an array of dislocations.

Since alkali halide crystals commonly designated "pure" contain concentrations of divalent cations of the order of  $10^{-6}$ , it is important to consider their effect on the grain boundary charge. Kliever and Koehler<sup>32</sup> have shown that when divalent cations are present in the crystal, they strongly influence the magnitude and nature of the dipole layer. At sufficiently high temperatures where the concentrations of thermally activated vacancies are much greater than divalent cation concentration, the situation is essentially the same as for the pure crystal. But at lower temperatures, the concentration of thermally activated vacancies decreases and the relative concentration of divalent

cations becomes appreciable. If the divalent cation impurities had no effect on the bulk cation vacancy concentration and thus on the dipole potential, the crystal would develop a net positive charge. This is prevented by an increase in the overall cation vacancy concentration which in turn causes a corresponding decrease in the potential across the space charge region.

With a further decrease in temperature, the magnitude of the space charge and the potential of the dipole layer continue to decrease until they finally go to zero and thus the grain boundaries, surfaces and dislocations become uncharged at that temperature. The temperature at which this occurs is called the isoelectric temperature ( $T_0$ ) because it is here that the innate difference between concentrations of anion and cation vacancies is precisely equal to the concentration of free impurities,<sup>32</sup> or

$$Ne^{-F^+/kT_0} - Ne^{-F^-/kT_0} = n_{if} \Big|_{T=T_0}, \quad (1)$$

where  $N$  is the total number of lattice sites per unit volume,  $F^+$  and  $F^-$  are the free energies of formation of cation and anion, respectively, and  $n_{if}$  is the density of unassociated divalent cation impurities.

For temperatures less than  $T_0$ , the anion vacancy concentration becomes negligible in comparison to the cation vacancies. As the temperature is reduced below  $T_0$ , the cation vacancies will continue to precipitate on the linear and planar defects of the crystal (which act as vacancy sinks due to falling temperature) since the tendency is to maintain a concentration based solely on thermal considerations. This precipitation of negative charge will attract positively charged divalent impurities (the only remaining source of positive charge) and the result will be a low temperature electrical dipole layer in the vicinity of the vacancy "sinks" which consists of excess cation vacancies on the vacancy sinks and a space charge layer in the adjacent bulk consisting primarily of divalent cation impurities. The dipole potential thus developed decreases the effective free energy of formation for cation vacancies, thereby making further precipitation energetically unfavorable and preserving bulk neutrality.

Kliewer and Koehler's theory<sup>32</sup> is particularly helpful in interpreting the results of the present investigation because of its predictions concerning the number and density of defects and the dipole potential in the region of a grain boundary. They have developed mathematical expressions showing the variations of the above quantities with temperature and divalent cation concentration. The variation of the dipole

potential with temperature and the divalent impurity content is well depicted in Figure 3 of their paper.<sup>32</sup> It is shown in the same figure that the isoelectric temperature of grain boundaries (dislocations and surfaces) in NaCl increases with an increase in the divalent cation concentration.

According to Kliewer and Koehler, the grain boundary region can be treated as composed of a core region and a surrounding space charge region in the lattice. The grain boundary core region in NaCl,<sup>38</sup> as also in the case of metals,<sup>39</sup> is assumed to be of the order of 2 to 3 atomic diameters and this width is assumed to be independent of both temperature and divalent cation concentration. The magnitude of the charge on the grain boundary core can be obtained from the equation derived by Kliewer and Koehler for the surface charge obtained by putting two surface solutions back to back.<sup>30</sup> The charge on the internal surface being  $Q' = 2Q$ . This charge changes with temperature and divalent cation concentration in the manner described earlier. The charge density in the space charge region can also be calculated from an equation developed theoretically by Kliewer and Koehler. The sign of this space charge varies with temperature and divalent cation concentration in a manner exactly opposite to that of the grain boundary or surface charge.

### B. Bulk Diffusion Coefficient

The diffusion coefficient for an isolated ion in a pure NaCl-type lattice is given by<sup>24</sup>

$$D = 4fa^2n\omega, \quad (2)$$

where  $f$  is the correlation factor<sup>40</sup> introduced to account for the fact that successive jumps of the tracer ion are not random but correlated,  $a$  is the anion-cation distance,  $n$  is the mole fraction of vacancies in the lattice and  $\omega$  is the probability per unit time that a vacancy will jump from one particular site to another.

An expression for the jump probability of ions in ionic solids has been derived using several different approaches,<sup>41</sup> e.g., absolute rate theory, many body theory of equilibrium statistics, and the dynamical theory of diffusion. All these derivations have resulted in an expression of the following form

$$\omega = \nu \exp(-\Delta g/kT), \quad (3)$$

where  $\Delta g$  is the height of the free energy barrier the ion must surmount to pass to the adjacent vacant site and  $\nu$  is an effective vibration frequency of the ion in the initial site.

The vacancy concentrations in NaCl-type lattice are given by

$$n_a n_c = \exp(-g_s/kT) = n_o^2, \quad (4)$$

where  $n_a$  and  $n_c$  are the anion and cation vacancy concentrations,  $n_o$  is the fractional concentration of Schottky defects, and  $g_s$  is the free energy of formation of a Schottky defect. On substituting the appropriate expressions for  $\omega$  and  $n$  in Eq. (2), it can be written in the familiar form

$$D = D_o \exp(-Q/kT), \quad (5)$$

where  $Q$ , the activation energy, is the sum of the enthalpies of vacancy formation and motion while  $D_o$  is the frequency factor.

For actual diffusion experiments, phenomenological diffusion equations are used to calculate single crystal diffusion coefficients. For a thin film source configuration of the type used in the present investigation, the solution of the one dimensional diffusion equation for the bulk diffusion (assuming film thickness  $h \ll Dt$ , where  $t$  is the diffusion time) is of the form,<sup>42</sup>

$$C = \frac{C_o h}{\sqrt{\pi Dt}} \exp(-x^2/4Dt), \quad (6)$$

where  $C$  is the concentration of the diffusing particles in the single crystal at a distance  $x$  from the surface



and  $C_0$  is the initial concentration of the radioactive source deposited on the single crystal sample.

The bulk diffusion coefficient can be obtained by assuming  $C$  proportional to the radioactivity of a thin slice of the crystal at a distance  $x$  from the surface of the crystal on which the tracer is originally deposited. A plot of the logarithm of the radioactivity  $C$  (counts per unit time) versus  $x^2$  is made. From Eq. (6) it is seen that this is a straight line of slope  $(4Dt)^{-1}$  so that if  $t$  is known,  $D$  can be calculated.

### C. Grain Boundary Diffusion Coefficient

In grain boundary diffusivity studies, the quantity determined experimentally is  $D'\delta$ , the product of the grain boundary diffusivity and the grain boundary width, because it is almost impossible to make an independent determination of  $\delta$ . Although a large number of different solutions<sup>43-48</sup> have been proposed for the grain boundary diffusion problem in the literature, only the approximate solution by Fisher<sup>43</sup> can be used directly and more conveniently.

According to the Fisher solution, as applied to the grain boundary diffusion measurements using a sectioning technique, the concentration of the tracer,  $\bar{C}$ , present a distance  $x$  from the surface is an experimentally determined quantity and is given by

$$\bar{C} = 4 \left( \frac{Dt}{\pi} \right)^{\frac{1}{2}} C_0 \exp \left[ \frac{-\sqrt{2}x}{(\pi Dt)^{\frac{1}{4}} (D'\delta/D)^{\frac{1}{2}}} \right], \quad (7)$$

where  $C_0$  is the concentration of the radioactive source initially deposited on the surface of the bicrystal sample. The quantity  $D'\delta$  can be obtained by assuming  $\bar{C}$  proportional to the specific activity of a slice of bicrystal at a distance  $x$  from the surface on which the source is originally deposited. A plot of logarithm of  $\bar{C}$  versus  $x$  is made. The linear part of these plots, based on Eq. (7) will have a slope,

$$m = \frac{-\sqrt{2}}{(\pi Dt)^{\frac{1}{4}} (D'\delta/D)^{\frac{1}{2}}}. \quad (8)$$

Experimentally determined values of  $m$ ,  $t$  and  $D$  can be used to calculate  $D'\delta$

$$D'\delta = \frac{1.128(D/t)^{\frac{1}{2}}}{m^2}. \quad (9)$$

In interpreting the grain boundary diffusivity results in metals,  $D'\delta$  is assumed to obey a relationship of the form

$$D'\delta = (D'\delta)_0 \exp(-Q_b/kT), \quad (10)$$

where  $Q_b$  is the "activation energy" of grain boundary diffusion and  $(D'\delta)_0$  is the pre-exponential factor. In alkali halides, however, because of comparatively few published experimental results, this assumption has not been fully tested for a wide enough temperature range. Riggs<sup>1</sup> showed that a relationship of the above form for  $D'\delta$  exists for chlorine ion diffusion in grain boundaries of NaCl for a temperature range of 420°C to 480°C.

#### IV. EXPERIMENTAL PROCEDURES

##### A. Crystal Growing

Single and bicrystals were grown in an NRC Model 2804A Czochralski type crystal growing furnace using the technique of Fuschillo, Nelson and Gimpl.<sup>49</sup> Harshaw's optical grade NaCl (see Table I) was used to grow "pure" crystals. High purity alumina crucibles were used for melting of the salt charge. These crucibles were precleaned and fired at 1100°C for 24 hours and were leached with molten high purity NaCl prior to actual use.

Single crystals were grown in the laboratory for bulk diffusion studies and for getting large enough seeds for growing the bicrystals. The techniques used for growing single and bicrystals were essentially identical except for the difference in the original seed configurations in the two cases. For single crystals, rectangular parallelepipeds were cleaved from the crystal cuttings supplied by Harshaw so that (100) planes were perpendicular to the four-fold axis. The parallelepiped was fastened to the pulling rod of the Czochralski crystal puller using platinum wire. Care was taken to make the four-fold axis coincident with the axis of rotation of the rod to ensure that the crystal grew straight. For growing tilt bicrystals, a stainless steel chuck with exactly half of the

TABLE I

## TYPICAL ANALYSIS OF HARSHAW SODIUM CHLORIDE

<u>IMPURITY</u>	<u>CONCENTRATION (ppm)</u>
Al	6
Ca	3
Cu	1
Fe	2
Mg	1
Si	2
	<hr/>
	15 ppm

intended angle machined on each side of a wedge was used. Two identical seeds, like the one for the single crystal growing, were held flush against the wedge in the center by two exterior clamping bars. This whole chuck assembly was attached to the bottom of the pulling rod of the crystal grower.

The NaCl crystal cuttings supplied by Harshaw were washed in deionized water and methanol, dried in a stream of hot air and then placed directly in a precleaned and prefired alumina crucible. Any residual traces of moisture were removed by preheating of the crucible and the charge under vacuum in the crystal grower at 400°C for about one hour. The salt was then melted in an atmosphere of prepurified 99.996% argon gettered with 87 at.% Zr-13 at.% Ti. Once molten, the salt was allowed to "equilibrate" for about two hours at 20°C above the growth temperature. The seeds were then immersed 0.1 in. in the molten salt and after the tips of the seeds were molten, they were allowed to rotate for about ten minutes to completely remove all polycrystalline growth on them. The temperature was then lowered to the growth point of the salt. The two seeds were allowed to grow together, forming the grain boundary and then the vertical growth of the bicrystal was initiated by starting the pull motion. Initially the pulling rates were kept very low, but once the bicrystal had grown to the desired

cross section, pulling rates were gradually increased. The crystal and the crucible were both rotated during the growth of the bicrystals to get a radially symmetric temperature gradient in the system. The growth of the bicrystal was terminated after a suitable size of the crystal was obtained by slightly raising the crystal above the bath surface and the furnace was cooled at a rate of about  $2^{\circ}\text{C}$  per minute. Bicrystals of about  $1 \times 1 \times 2$  in. size were grown in the present study. Spectroscopic examinations showed that no detectable impurity was introduced during the crystal growth procedures.

A systematic procedure was followed to get a desired doping level of about 150 ppm  $\text{CaCl}_2$  in the doped bicrystals. The phase diagrams for  $\text{NaCl-CaCl}_2$  system available in the literature<sup>50</sup> give a crude estimate for the distribution coefficient ( $K$ ). Therefore, initially, a trial bicrystal was grown by using the reported  $K$  value of  $1/9.88$ . The concentration of  $\text{CaCl}_2$  in the trial bicrystal as determined by atomic absorption was observed to be 560 ppm thereby indicating a  $K$  value of  $1/2.65$ . A new bicrystal was grown from a fresh bath with  $\text{CaCl}_2$  concentration corresponding to the observed distribution coefficient. Cuttings taken from different sections of this bicrystal were analyzed and the results (see Table II) showed an average  $\text{CaCl}_2$  concentration of

TABLE II

ANALYSIS OF SODIUM CHLORIDE BICRYSTAL  
DOPED WITH CALCIUM CHLORIDE

<u>SAMPLE</u>	<u>CALCIUM CHLORIDE (ppm)</u>
A	143.9
B	137.1
C	147.7
D	143.3



142±5 ppm. No significant concentration gradients were observed in the bicrystal.

Fisher's reagent grade anhydrous calcium chloride and Harshaw's NaCl were used to grow the doped bicrystals. The salt bath for the doped bicrystals was prepared by stirring the molten charge for about 24 hours under argon atmosphere to allow complete mixing of the charge. Both "pure" and doped bicrystals contained 45° (100) planar symmetric tilt grain boundaries.

#### B. Sample Preparation, Sectioning, Counting and Autoradiography

The samples used for bulk diffusion measurements were parallelepipeds cleaved from the single crystal boule with a typical size of  $5/8 \times 3/8 \times 1/16$  in. The samples containing a symmetrical tilt grain boundary were cleaved from the bicrystalline boule and were similar in size to the single crystal samples but pentagonal shaped (see Fig. 2) because of the misorientation of the (100) planes in the two adjoining crystals forming the grain boundary. The samples were initially flattened with an American Optical Spencer Model 860 microtome. The upper surface of a detachable sample mounting block was permanently aligned parallel to the plane of movement of the microtome knife edge by using a binocular microscope. Salol was used to hold

the samples firmly on the mounting block and after flattening, it was removed by washing the sample in acetone and then toluene.

In the present investigation, the radioisotope  $^{131}\text{I}$  was used as a tracer for both bulk and grain boundary diffusivity measurements. It was received as  $\text{Na}^{131}\text{I}$  in 0.1N NaOH solution with a concentration of about 250 millicurie per milliliter. This solution was diluted with deionized water and then neutralized to a pH of 8 using an  $\text{NH}_2\text{OH}\cdot\text{HCl}$  solution. Diffusion couples were prepared by vapor deposition of the isotope from a platinum crucible using a tantalum heating coil in an NRC vacuum evaporator at a pressure of less than  $3 \times 10^{-6}$  torr. The evaporated layer thickness on the samples was about  $3 \times 10^{-6}$  cm with a total isotope activity of about 200 microcurie. Following the evaporation procedure, each sample was wrapped in platinum foil, encapsulated in a vycor ampule at a pressure of less than  $5 \times 10^{-6}$  torr, and then put in the furnace for diffusion annealing. The temperature of the furnace was controlled to  $\pm 0.05^\circ\text{C}$ . The short-time temperature fluctuations in the annealing furnaces were observed to be negligible while the long-time temperature stability was always better than  $\pm 1^\circ\text{C}$ . The spatial variation of temperature over the volume occupied by the sample was always less than  $0.5^\circ\text{C}$ . The

temperature was measured with a chromel-alumel thermocouple which was placed in contact with the outer surface of the ampule.

After annealing, the diffusion profiles of the samples were obtained by microtome sectioning and measuring the section activity. If the pre-flattened sample suffered no deformation during the annealing run, it could be repositioned on the sample holder of the microtome without any misalignment of its top surface with respect to the knife edge. Before sectioning, the sides of the annealed sample were cleaved off to remove any surface diffusion effects. An autoradiograph of the sample was taken at this stage to make sure that no radioactive debris were left on the sides of the sample due to cleaving. Any deformation caused by cleaving was removed by grinding the back of the sample and the resulting misalignment of the sample surface during sectioning was always observed to be less than 4 microns per cm. The sections for counting were obtained by first painting the top sample surface with a solution of Duco Cement in 2-pentanone, allowing the solution to dry, and then slicing off the sample surface with the microtome. The resulting sample section, consisting of a very thin layer of Duco Cement to which the powdered salt adhered, formed a compact, cigar-shaped roll which furnished a very reproducible counting geometry. Self absorption

does not constitute a source of error for this counting geometry as gamma radiations are being counted for the isotope  $^{131}\text{I}$ . A slice thickness of 4 microns for the single crystal samples and 10 microns for the bicrystal samples was generally used.

A scintillation counter was used to determine the activities of the sections containing  $^{131}\text{I}$ . The  $^{131}\text{I}$  spectrum between 0.332 and 0.372 MeV was counted and the background rate for this range was 3 cpm. As  $^{131}\text{I}$  isotope has a half life of only 8.05 days, the elapsed times between counting of the first section and the remaining sections of each sample were duly recorded and the counting rates were then corrected for the loss in activity due to the radioactive decay.

During different stages of sectioning of the samples, autoradiographs were taken to insure that the section activities being counted were only due to the isotopes that had diffused through the sample either through the bulk or along the grain boundary. Figs. 1 and 2 show the  $^{131}\text{I}$  penetration profile and accompanying autoradiographs for a typical "pure" bicrystal sample. The enhanced grain boundary diffusion is very clearly seen in the autoradiographs.

### C. Experimental Data and Estimation of Errors

For single crystal diffusion, the logarithm of the radioactivity of a section in counts per minute was

Figure 1.  $^{131}\text{I}$  Iodine Penetration Profile of a  
"Pure" Bicrystal Sample Showing the  
Bulk and Grain Boundary Diffusion.

Annealed for  $1.405 \times 10^5$  sec. at  
539.5°C.

The numbered positions 1 through 4  
indicate the depth where the  
autoradiographs of Figure 2 were taken.

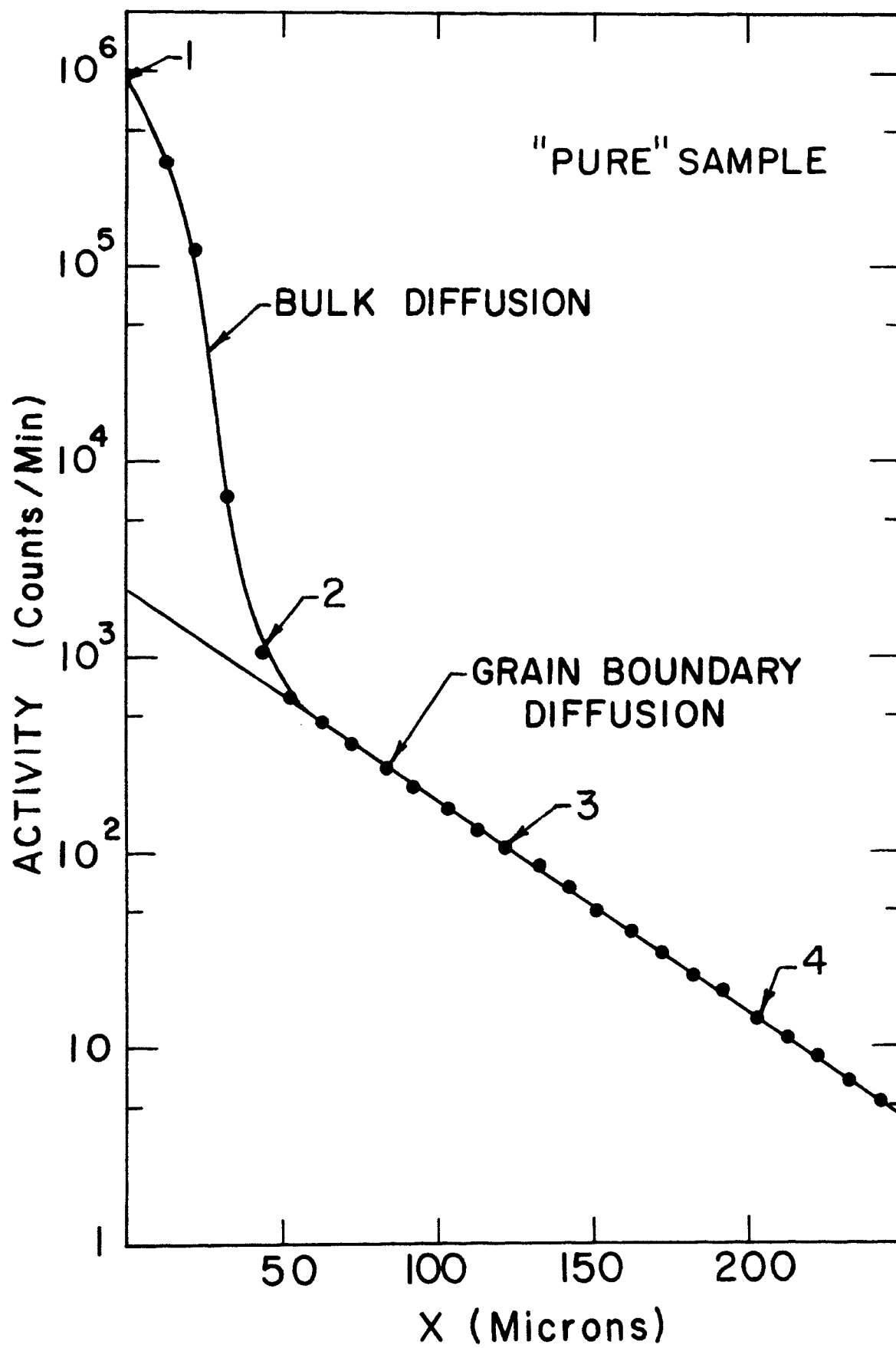


FIGURE 1

Figure 2. A Typical Series of Autoradiographs of the Bicrystal Diffusion Sample of Figure 1 Taken During Sectioning at Various Penetration Depths.

- #1. Original evaporated surface after diffusion anneal
- #2. 42 microns from original sample surface
- #3. 132 microns from original sample surface
- #4. 212 microns from original sample surface

The photographs are positive prints of the original autoradiographic negatives.

AUTORADIOGRAPHS



#1



#2



#3



#4

FIGURE 2



plotted against  $x^2$ . These plots were generally linear over two to five decades of count values (see Fig. 3). The best line for each set of log (counts per minute) versus  $x^2$  data was determined by the least squares method. The slope of the line and Eq. (6) were used to calculate the diffusion coefficient,

$$D = \frac{\ln C_1 - \ln C_2}{4(x_2^2 - x_1^2) 10^{-8} t}, \quad (11)$$

where  $(C_1, x_1^2)$  and  $(C_2, x_2^2)$  are the coordinates of the two points of the best line, with  $x$  being in microns and  $t$ , the measured diffusion time in seconds.

Fisher's solution<sup>43</sup> was preferred for determining the grain boundary diffusion coefficients in the present investigation, because when it is applied to sectioning techniques it causes small but correctible errors in the measured values of  $D'\delta$  and almost negligible errors in the measured activation energies of diffusion.<sup>51</sup> As the corrections to the measured values of  $D'\delta$  due to application of Fisher's solution to the present study were found to be within the limits of experimental uncertainty, the data for "pure" and doped NaCl bicrystal samples were analyzed using the Fisher solution with no correction for the formalistic error.

For determining  $D'\delta$ , the logarithm of the radioactivity of a section of bicrystal in counts per minute

Figure 3. A Typical  $^{131}\text{I}$  Iodine Penetration Profile  
of a Single Crystal Sample.

Annealed for  $1.324 \times 10^5$  sec. at  $560.5^\circ\text{C}$ .

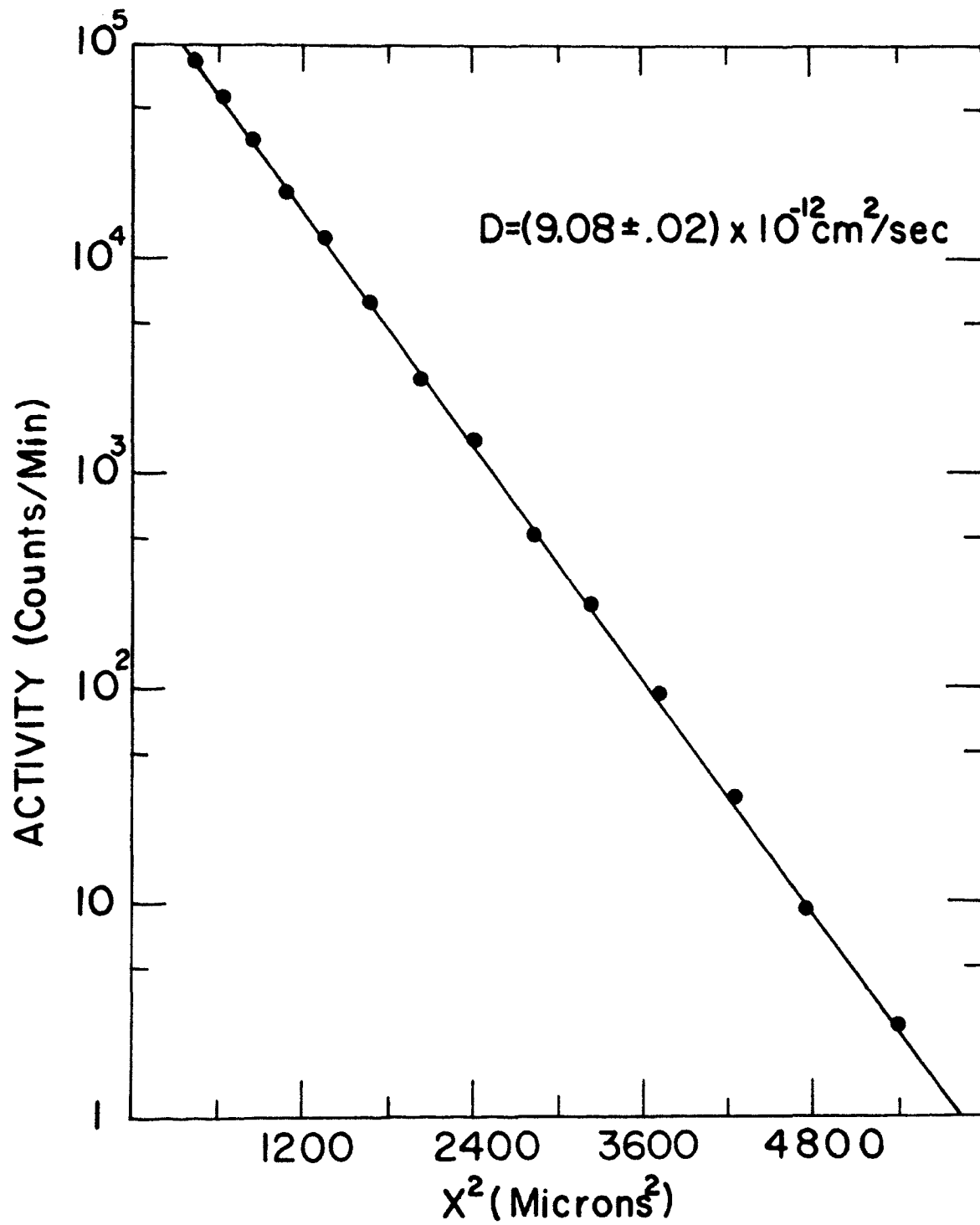


FIGURE 3

was plotted against  $x$ . These plots were linear over one to three decades of count values (see Figs. 1 and 4). The linear region in these plots indicates the contribution to diffusion due to the grain boundary alone while the initial curved region is due to both the bulk and the grain boundary diffusion. The best line for the linear region was determined by the method of least squares. The slope of the linear region and Eq. (9) were used to calculate  $D'\delta$

$$D'\delta = 1.128 (D/t)^{\frac{1}{2}} \frac{(x_2 - x_1)^2 \times 10^{-8}}{(\ln C_1 - \ln C_2)^2}, \quad (12)$$

where  $(C_1, x_1)$  and  $(C_2, x_2)$  are the coordinates of the two points of the best line. Using earlier experimentally determined values of  $D$ ,  $D'\delta$  was calculated for each sample.

The temperature stability of the annealing furnaces was determined by repeated measurements of temperature for each sample in any particular furnace. It was observed that the precision of temperature measurements was always better than  $\pm 1^\circ\text{C}$ . The accuracy of the annealing temperature, as measured by a chromel-alumel thermocouple, was found to be  $\pm 1^\circ\text{C}$ . Therefore, the total uncertainties in the measured values of  $D$  and  $D'\delta$  were determined by

Figure 4. A Typical  $^{131}\text{I}$  Iodine Penetration Profile  
of a  $\text{CaCl}_2$  Doped ( $142 \pm 5$  ppm) Bicrystal  
Sample.

Annealed for  $1.252 \times 10^5$  sec. at  
 $560.1^\circ\text{C}$ .

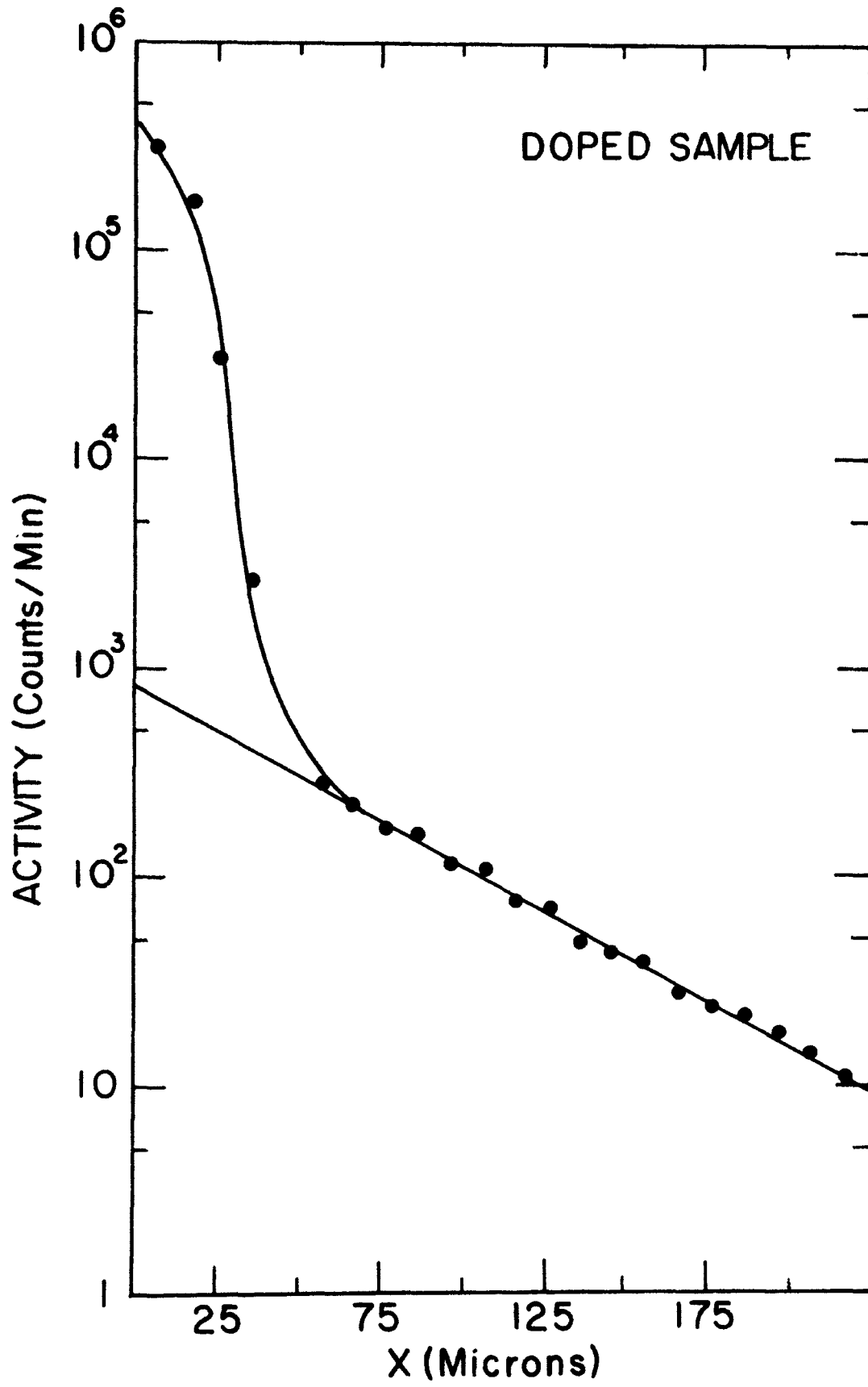


FIGURE 4

$$\frac{\Delta D}{D} = \frac{Q}{kT^2} \Delta T. \quad (13)$$

These were found to be approximately 4.5% for  $^{131}\text{I}$  bulk diffusivities and 2.5% for grain boundary diffusivities.

The systematic error in the value of  $D$  because of the finite section thickness, sectioning misalignment distance, and the evaporation layer thickness is given by<sup>52</sup>

$$D_{\text{true}} = D_{\text{experimental}} \left( 1 - \frac{d^2 + s^2 + 4h^2}{24Dt} \right), \quad (14)$$

where  $d$  is the section thickness,  $s$  is the misalignment distance (the misalignment distance is equal to the product of the crystal width and the misalignment angle, for small angles), and  $h$  is the evaporation layer thickness. The systematic error thus calculated for bulk diffusion was always found to be less than 1.2%. However, in grain boundary diffusion, where the logarithm of the section activity of a sample is assumed to be proportional to  $x$ , Shirn, Wajda and Huntington<sup>53</sup> showed that an analysis of the type which leads to Eq, (14) yields no systematic error in the measured values of  $D'\delta$  due to the section thickness and slicing misalignment distance.

Errors in time measurement were quite small. Errors in the measurement of diffusion time are caused due to the non-ideal heating and cooling conditions in starting

and terminating a diffusion anneal. Since the diffusion times for the single and bicrystal samples ranged from  $1.2 \times 10^5$  to  $2 \times 10^6$  seconds, the heating and cooling times for any sample were kept less than 1% of the total diffusion time.

The random errors from statistical fluctuations in the counting rate were kept low by counting at least 1000 counts on any slice and by continuing counting only in slices whose counting rates were about twice the background count. Values of  $D$  and  $D'\delta$  and their 95% confidence limits were obtained by fitting the single and bicrystal data to Eqs. (6) and (7) by the method of least squares using a computer program. The uncertainties in the values of  $D$  due to the error in the slope and in the diffusion time measurement were determined by

$$\frac{\Delta D}{D} = \left| \frac{\Delta t}{t} \right| + \left| \frac{\Delta m}{m} \right|. \quad (15)$$

Eq. (12) was used to determine the uncertainties in the values of  $D'\delta$  due to the above two factors to get

$$\frac{\Delta(D'\delta)}{D'\delta} = \frac{1}{2} \left| \frac{\Delta t}{t} \right| + 2 \left| \frac{\Delta m}{m} \right|. \quad (16)$$

Values of  $m$  used in Eqs. (15) and (16) were the ones determined by the computer program. The total error limit in the values of  $D$  was found to be 5% while the



error limit for all values of  $D'\delta$ , on the average was observed to be approximately  $\pm 10\%$ .

## V. EXPERIMENTAL RESULTS

### A. Single Crystal Diffusion Coefficients

The iodine bulk diffusion coefficients for single crystals of "pure" and calcium chloride doped sodium chloride are shown as functions of temperature in Fig. 5. The  $^{131}\text{I}$  diffusion coefficient in "pure" sodium chloride is well represented by

$$D = (504 \text{ cm}^2/\text{sec}) \exp(-2.27 \text{ eV}/kT) \quad (17)$$

over the temperature range investigated. These results are in very good agreement with those of Beaumont and Cabane<sup>13</sup> for sodium chloride of similar purity

$$D = (500 \text{ cm}^2/\text{sec}) \exp(-2.23 \text{ eV}/kT). \quad (18)$$

Chemla<sup>2</sup> observed an activation energy value of 2.29 eV and the same value for the frequency factor as that of Beaumont and Cabane.

Because of such good agreement for the iodine single crystal diffusion coefficient measurements of "pure" NaCl with those of other authors, it was decided not to repeat single crystal diffusion work for doped NaCl but to use the data available in the literature. A number of investigators<sup>5,11,12</sup> have measured anion diffusion coefficients in sodium chloride and they all seem to agree with the main conclusions of Laurance<sup>5</sup> that single

Figure 5. Arrhenius Plots of  $^{131}\text{I}$  Iodine Single  
Crystal Diffusion Coefficients for  
"Pure" and  $\text{CaCl}_2$  Doped Sodium  
Chloride.

The doped plot is based on results  
of Neal Laurance.<sup>5</sup>

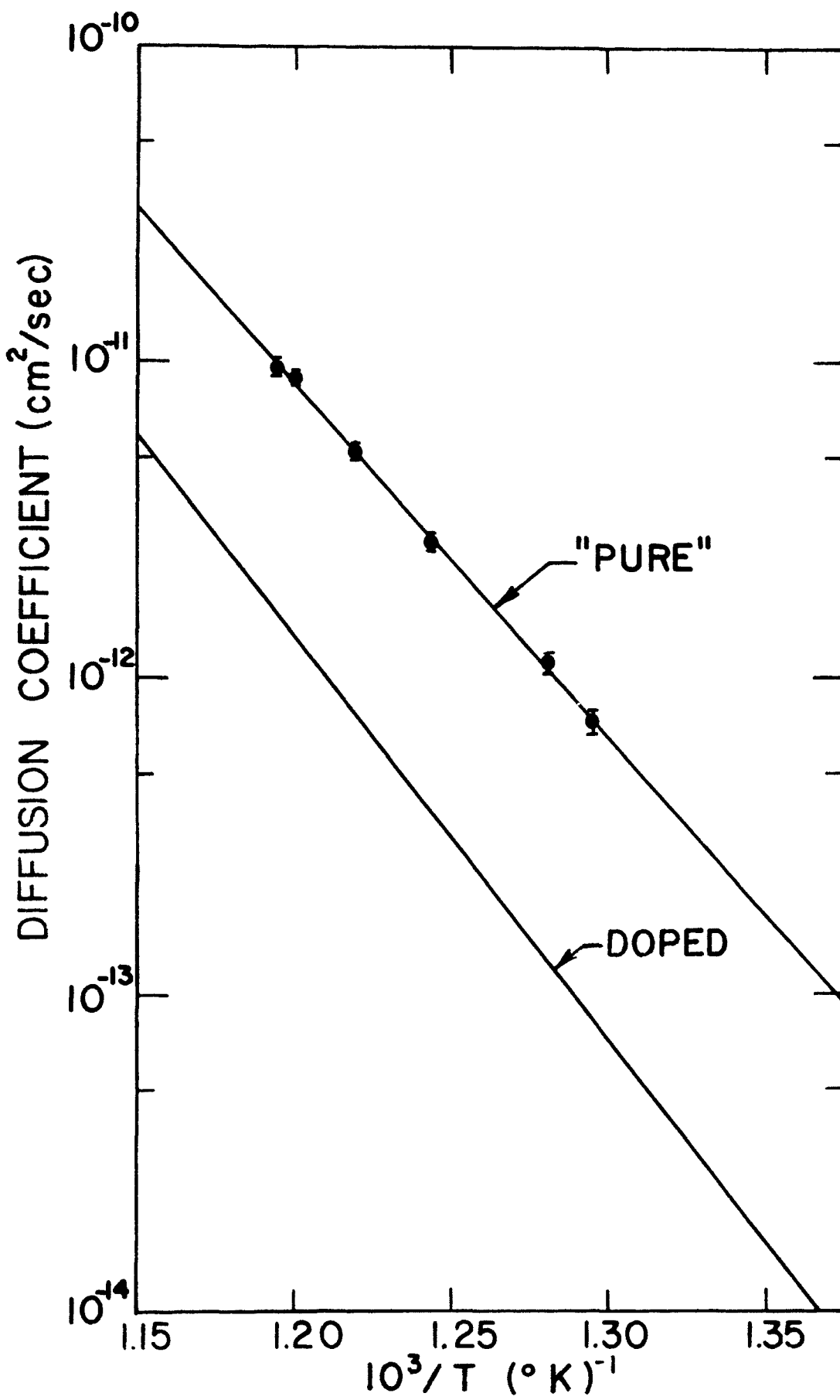


FIGURE 5

vacancies are responsible for diffusion in pure single crystals while the vacancy pair mechanism dominates the diffusion process in doped crystals. Laurance varied calcium chloride dopant from 100 to 1000 ppm and reported that the diffusion coefficient in the doped crystals is lowered but this decrease is insensitive to the differences in calcium concentration. Also, activation energy values of  $^{36}\text{Cl}$  and  $^{131}\text{I}$  for single crystal diffusion in pure NaCl are reported to be about the same.<sup>13,54</sup> It was therefore decided to assume the proportional decrease in iodine diffusion coefficient due to doping to be the same as that reported by Laurance for chlorine diffusion in the doped single crystals. The lower solid curve shown in Fig. 5 is obtained in this manner and can be represented by

$$D = (1421.4 \text{ cm}^2/\text{sec}) \exp(-2.48 \text{ eV}/kT). \quad (19)$$

This procedure seems satisfactory as the main results of the present study, namely the anomalous behavior in the  $\ln D'\delta$  vs  $1/T$  plots, are not affected qualitatively and only weakly quantitatively, as seen later in the Discussion.

#### B. Grain Boundary Diffusion Coefficients

The iodine grain boundary diffusivity data in NaCl bicrystals showed a very unusual shape of the curves in

In  $D'\delta$  vs  $1/T$  plots in comparison with the usual linear behavior expected in the case of metals (see Fig. 6). It is important to note that both the curves in this figure show identical principal features. Fig. 7 represents a schematic diagram of four major temperature regions, marked I through IV, observed in both "pure" and the doped bicrystal diffusivity plots of Fig. 6. The minima in the  $\ln D'\delta$  vs  $1/T$  plots of "pure" and doped bicrystal samples occur at  $519^\circ\text{C}$  and  $493^\circ\text{C}$ , respectively. Regions I through III are quite distinct while the transition between regions III and IV is very gradual.

In region I, the iodine grain boundary diffusion coefficients were found to satisfy a relationship of the form shown in Eq. (10). Pre-exponential factor  $(D'\delta)_0$  and the activation energy  $Q_b$  were calculated from Fig. 6 and are given in Table III.

The values of  $D'\delta$  were observed to be between  $10^{-14}$  and  $10^{-13}$   $\text{cm}^3/\text{sec}$  for the "pure" and between  $10^{-16}$  and  $10^{-15}$   $\text{cm}^3/\text{sec}$  for the doped bicrystal, for the entire temperature range studied ( $430^\circ\text{C}$  to  $570^\circ\text{C}$ ). Values of bulk diffusion  $D$  in the same temperature range vary between  $10^{-14}$  and  $10^{-11}$   $\text{cm}^2/\text{sec}$  for the "pure", and between  $10^{-15}$  and  $10^{-12}$   $\text{cm}^2/\text{sec}$  for the doped single crystals. The exact width of the grain boundary core region in NaCl is not known; however, it is reasonable

Figure 6. Plots Showing the Variation of the  $^{131}\text{I}$  Iodine Grain Boundary Diffusion Parameter,  $D'\delta$ , With Temperature for "Pure" and  $\text{CaCl}_2$  Doped ( $142 \pm 5$  ppm) Sodium Chloride Bicrystal Samples.

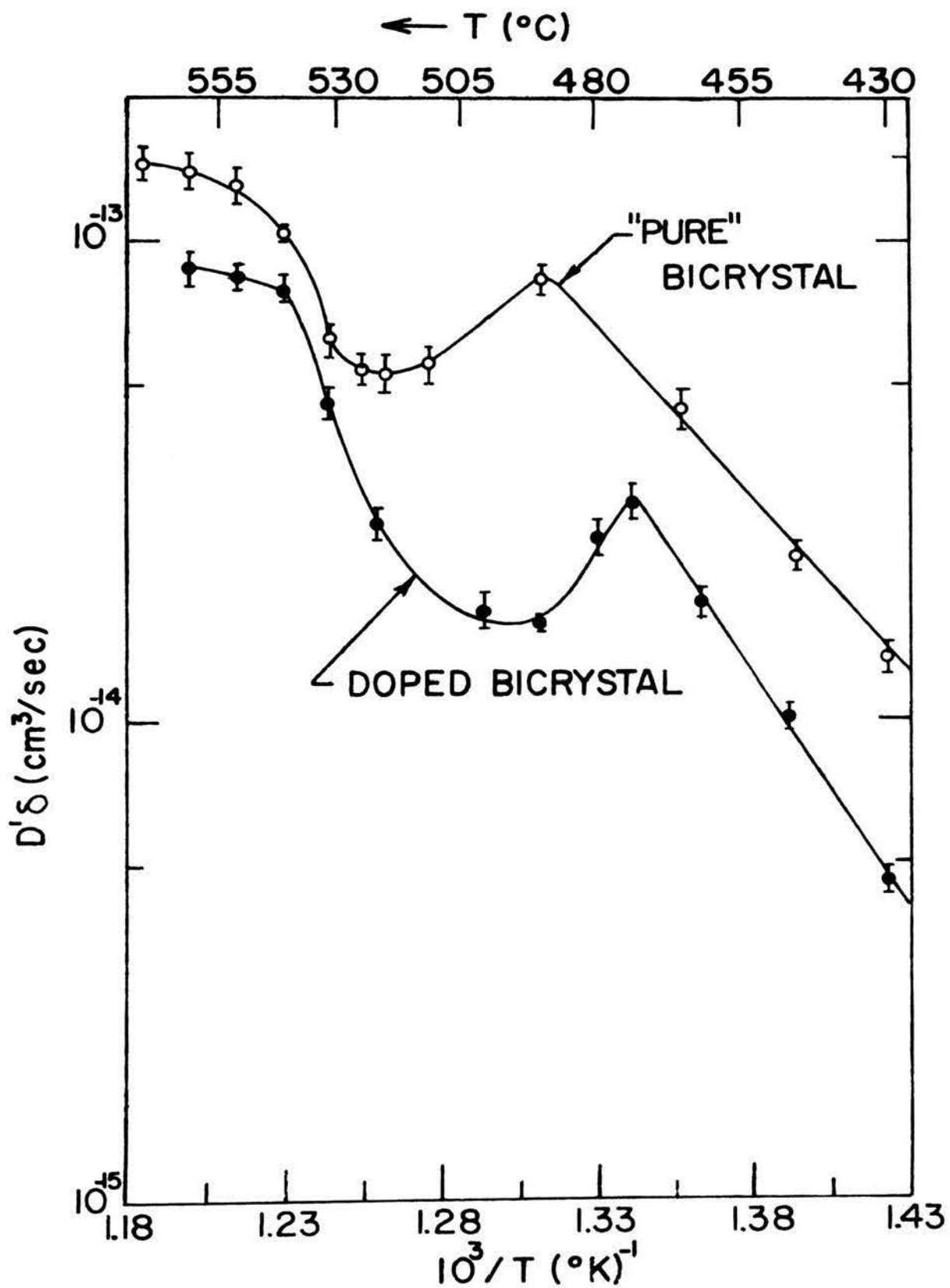


FIGURE 6



Figure 7. A Schematic Sketch of the  $\ln D'\delta$  vs  $1/T$  Plots Shown in Figure 6.

The numbered regions I through IV are typical of the plots shown for "pure" and doped bicrystals in Figure 6.

A is defined in the text.

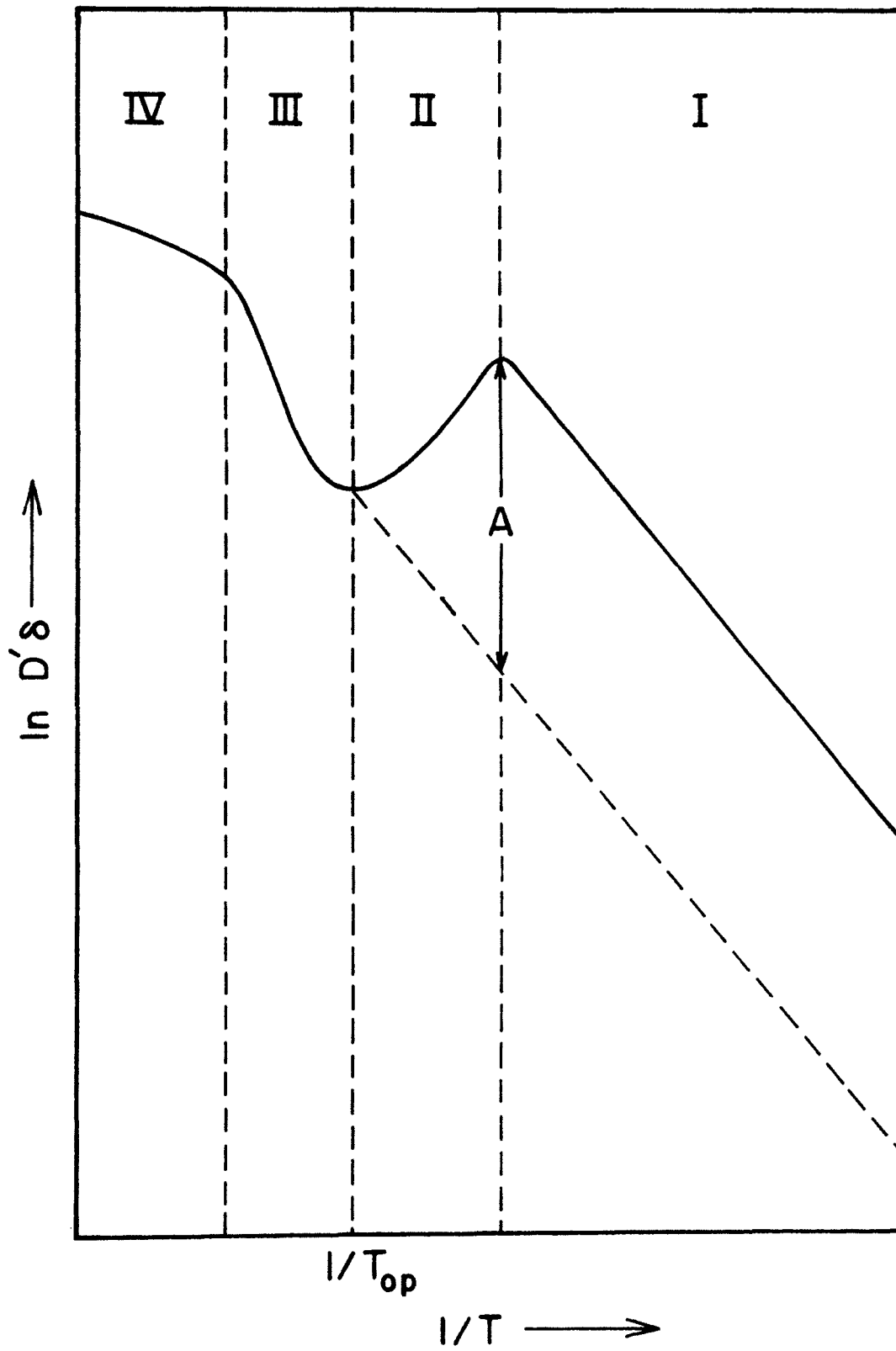


FIGURE 7

TABLE III

ACTIVATION ENERGIES AND PRE-EXPONENTIAL FACTORS  
OF IODINE GRAIN BOUNDARY DIFFUSION

<u>BICRYSTAL</u>	<u>ACTIVATION ENERGY OF <math>^{131}\text{I}</math> GRAIN BOUNDARY DIFFUSION <math>Q_b</math> (eV)</u>	<u>PRE-EXPONENTIAL FACTOR <math>(D'\delta)_0</math>, <math>\text{cm}^3/\text{sec}</math></u>
"pure"	1.36	$8.45 \times 10^{-5}$
$\text{CaCl}_2$ Doped ( $142 \pm 5$ ppm)	1.93	0.39

to assume it to be in the range of  $10^{-7}$  cm- $10^{-8}$  cm on the basis of the results of Sun and Bauer<sup>38</sup> on NaCl and the reported range of grain boundary widths of metals.<sup>39</sup> Therefore the present results show an enhancement of diffusion owing to symmetrical tilt grain boundaries by a factor of  $10^5$  to  $10^7$  over the bulk diffusion in single crystals.

## VI. DISCUSSION

The 2.27 eV measured value of activation energy of iodine diffusion in "pure" NaCl single crystals agrees well with the sum of the free energies of formation and motion of an anion vacancy ( $1.11 + 1.11 = 2.22$  eV) in sodium chloride as shown in Table IV. This confirms the conclusions of earlier authors<sup>2,5,11-13</sup> that the single-vacancy mechanism is responsible for anion diffusion in pure single crystals of NaCl. The close agreement of the presently measured bulk diffusivity data with the data reported in the literature and the autoradiographs for the grain boundary diffusion (Fig. 2) indicate that the data acquired in the present study are of sufficient quality to warrant the following discussion.

The grain boundary diffusivity data follow an Arrhenius-type plot in the low temperature region I (see Figs. 6 and 7). Large deviations from Arrhenius-type behavior are observed in the high temperature regions II through IV and this is the key result of the present investigation. Any proposed mechanism for diffusion along the grain boundaries should explain the experimental observations of the enhanced diffusion of iodine in the grain boundary diffusivity data at higher temperatures in both the "pure" and calcium chloride doped bicrystals. The principal features observed in

TABLE IV

ENTHALPIES AND ENTROPIES OF FORMATION AND MOTION OF VARIOUS DEFECTS IN SODIUM CHLORIDE

DEFECT	ENTHALPY OF FORMATION (eV)	ENTROPY OF FORMATION (eV/°C)	ENTHALPY OF MOTION (eV)	ENTROPY OF MOTION (eV/°C)
Cation Vacancy Vacancy	1.07 <sup>55*</sup> 0.95 <sup>34</sup>	6.1 k <sup>55</sup>	0.80 <sup>56</sup>	3.1 k <sup>56</sup>
Anion Vacancy	1.05 <sup>55</sup> 1.17 <sup>34</sup>	0.1 k <sup>55</sup>	1.11 <sup>11</sup>	
Schottky Defect	2.12 <sup>56</sup>	6.2 k <sup>56</sup>	--	--
Vacancy Pair	1.27 <sup>11</sup>		Cation Jump 1.46 <sup>10</sup> Anion Jump 1.27 <sup>10</sup>	
Divalent Cation- Cation Vacancy Complex	0.6 <sup>56</sup>		Cation Jump 0.7 <sup>13</sup>	

\*Small numbers in this table refer to the reference numbers.

Fig. 6 could be due to either some intrinsic phenomenon at the grain boundaries or they could be extrinsic effects due to some foreign agent such as moisture present at the grain boundaries.

Cabane<sup>15</sup> in his earlier work on diffusion in polycrystalline alkali halides, reported some influence of moisture on diffusivity data of samples not prepared in a moisture free atmosphere. Since elaborate precautions were taken to exclude water from the sample environments of the present study, an extrinsic effect due to its presence on grain boundary diffusion seems unlikely. Also calcium ion impurities do not seem to be the cause of the observed diffusion anomalies because both "pure" and doped curves (Fig. 6) exhibit the same four major regions.

The failure of extrinsic effects to explain the observed results indicates that an intrinsic grain boundary phenomenon must be responsible for the observed grain boundary diffusion. In metals, where an Arrhenius-type plot is observed for grain boundary diffusion, the mass transport carriers are essentially point defects and the grain boundaries are uncharged. But in alkali halides like NaCl, electrically charged defects take part in the diffusion. It is also known that surfaces, dislocations and grain boundaries in NaCl are electrically charged. Hence it seems reasonable to look for an explanation of the observed diffusion anomalies in terms of the concept of

space charge theory in ionic crystals. Kliewer and Koehler's theory of charged defects in ionic crystals<sup>32</sup> and ionic polarization effects on anion diffusion as observed by Laurant and Benard,<sup>14</sup> when used to analyze the present results, seem to explain the present results satisfactorily. Kliewer and Koehler's theory essentially states that the dipole potential around the surfaces, dislocations and grain boundaries in NaCl becomes zero at the isoelectric temperature and the magnitude of the potential increases as the difference between the measuring temperature and the isoelectric temperature increases in either direction. Laurant and Benard observed that the increase in the diffusivity in polycrystalline alkali halides was directly proportional to the polarization of the anions.

It is essential to know the value of the isoelectric temperature for the material under study in order to determine the effect of the electrical dipole layer upon the grain boundary diffusion at a given temperature. Kliewer and Koehler's theory predicts an isoelectric temperature of an external surface or a dislocation to be approximately 300°C for NaCl of the purity investigated in the present work. Indirect measurements of the dislocation isoelectric temperature by the same authors,<sup>55</sup> based on internal friction results, yielded a value of about 460°C for NaCl. Thus their theory seems to only approximately predict the isoelectric



temperature. In contrast to these results, Davidge<sup>34</sup> reported a directly determined experimental value of 511°C for the dislocation isoelectric temperature in NaCl of the same purity as the "pure" bicrystal used in the present study. Although the structure of the large angle grain boundaries is not completely known, these boundaries still retain some characteristics of a dislocation structure even at maximum misorientation, as pointed out by Hoffman,<sup>25</sup> Smoluchowski<sup>26</sup> and Bishop.<sup>27</sup> It is therefore reasonable to believe that the dislocation isoelectric temperature in NaCl is close to the grain boundary isoelectric temperature in bicrystals of NaCl. In the present investigation, the minimum in the  $\ln D'\delta$  vs  $1/T$  curve in "pure" bicrystal occurs at 519°C which is about the same as the isoelectric temperature of NaCl reported by Davidge. The following discussion will therefore be based on the assumption that the temperature where the minimum in  $D'\delta$  is observed corresponds to the isoelectric temperature of NaCl, denoted by  $T_{op}$ .

The regions I through IV in the  $\ln D'\delta$  vs  $1/T$  plots (Fig. 6) then develop due to two competing effects acting simultaneously on the grain boundary diffusion in NaCl bicrystals. These two effects are the dipole potential due to the charge cloud around the grain boundary and the thermal activation. The combined influence of these two

effects on  $D'\delta$  varies in regions I through IV depending on the proximity of the region to the isoelectric temperature. A semi-quantitative explanation of these two effects on the grain boundary diffusivity plots can be given by deriving a general mathematical expression for  $D'\delta$ . This approach is independent of the mechanism of diffusion at the grain boundary.

The grain boundary can be assumed to be a continuum region like the bulk. The diffusivity in the bulk in NaCl is given by

$$D = \frac{fkT\mu n}{e}, \quad (20)$$

where  $\mu$  is the mobility of the diffusing ions,  $n$  is the mole fraction of the point defects and  $e$  is the electronic charge. Using Einstein's relationship, this expression can be shown to be equivalent to Eq. (2) shown earlier. If  $D'$  is the anion grain boundary diffusivity, then as in the bulk, it can be written as

$$D' = 4fa^2n'\omega', \quad (21)$$

where  $n'$  is the mole fraction of the negatively charged point defects while  $\omega'$  is the jump probability in the grain boundary region. Further,

$$\omega' = \nu \exp(-\Delta g'/kT), \quad (22)$$

where  $\Delta g'$  is height of the free energy barrier that the anion must surmount to pass to the next available site in the grain boundary. It is hypothesized that  $\Delta g'$  is composed of two components due to simultaneous presence of the thermal activation and the electrical effect at the grain boundary,

$$\Delta g' = \Delta g_o + \Delta g_e , \quad (23)$$

where  $\Delta g_o$  and  $\Delta g_e$  are the free energy barriers for the diffusion jump in the grain boundary due to the thermal and the electrical effects, respectively. Eq. (21) can therefore be written as

$$D' = 4fa^2vn'\exp(-\Delta g_o/kT)\exp(-\Delta g_e/kT). \quad (24)$$

As observed by Laurant and Benard, the electrical field influences the diffusivity mainly through the polarization of the anions. Thus, if  $\alpha$  is the polarizability of the diffusing anions and  $E$  is the electrical field strength of the dipole layer around the grain boundary, then

$$\Delta g_e = -\frac{1}{2}\alpha E^2. \quad (25)$$

Following Kliever and Koehler's treatment for calculations involving a free surface region, consider an electrically neutral crystal having free (100) surfaces at  $x = 0$  and

$x = 2L$  and of infinite extent in the  $y$  and  $z$  directions so that the problem becomes one dimensional. The electrical field is therefore given by

$$E = -\frac{d\Phi}{dx} = -\frac{1}{e} \frac{d(e\Phi)}{dx}, \quad (26)$$

where  $\Phi$  is the potential due to the electrical dipole layer around the surface. Expanding the last term in Eq. (24) in a series,

$$D' = 4fa^2vn'\exp(-\Delta g_o/kT) \left[ 1 + \frac{\alpha}{2e^2kT} \left\{ \frac{d(e\Phi)}{dx} \right\}^2 \right]. \quad (27)$$

A grain boundary can be treated as an interface composed by putting two external surfaces back to back and the charge on the grain boundary  $Q' = 2Q$ , where  $Q$  is the charge on the external surface of the same material.<sup>30</sup>

Therefore,

$$D' = 4fa^2vn'\exp(-\Delta g_o/kT) \left[ 1 + \frac{\alpha}{2e^2kT} \left\{ 2\frac{d(e\Phi)}{dx} \right\}^2 \right]. \quad (28)$$

If  $\delta$  is the grain boundary width, then

$$D'\delta = 4fa^2vn'\delta\exp(-\Delta g_o/kT) \left[ 1 + \frac{2\alpha}{e^2kT} \times \left\{ \frac{d(e\Phi)}{dx} \right\}^2 \right]. \quad (29)$$

Now one defines a normalized dipole potential  $z(x)$  and a normalized coordinate  $s$  as

$$z(x) = \{e\phi(x) - e\phi_\infty\}/kT \quad (30)$$

$$\text{and } s(x) = \kappa_+ x, \quad (31)$$

$$\text{where } \kappa_+^2 = \frac{8\pi N e^2}{\epsilon kT} \exp\{(e\phi_\infty - F^+)/kT\}. \quad (32)$$

$\phi_\infty$  is the value of the dipole potential in the bulk, where electrical charge neutrality exists.  $\kappa_+^{-1}$  is effectively the width of the space charge region in the temperature range of interest here. Kliever and Koehler in their paper, show that

$$z = 4 \tanh^{-1}\{e^{-s} \tanh(\frac{1}{4} z_0)\}, \quad (33)$$

$$\text{where } z_0 \equiv z|_{x=0} = -e\phi_\infty/kT. \quad (34)$$

The theoretical treatment of space charge theory in ionic crystals in the case of surfaces, dislocations and grain boundaries is very similar.<sup>30-32</sup> Therefore, as shown in Fig. 8, the potential  $\phi$  due to a dipole layer around the grain boundary is zero at the axis of the grain boundary core and it approaches a value  $\phi_\infty$  within the bulk where electrical neutrality exists. Kliever and Koehler have shown in Fig. 1 of their paper that the potential achieves its bulk value ( $\phi_\infty$ ) essentially

Figure 8. Sketch Showing Variation of  $e\phi$  with Distance  $x$  from the Grain Boundary Core Into the Bulk for Temperatures Other than the Isoelectric Temperature in Ionic Crystals.

$\kappa_+$  and  $\delta$  are defined in the text.

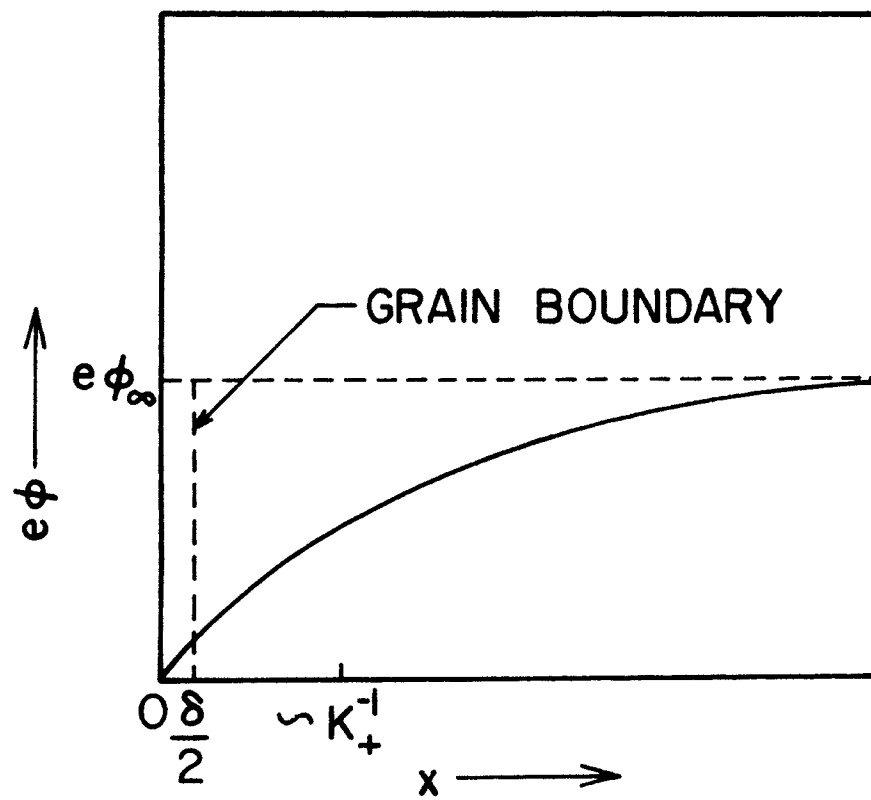


FIGURE 8

exponentially for  $|z_0| \leq 1$  and even more rapidly as  $z_0$  increases beyond 1. Thus to determine the value of the electrical field in the grain boundary, it is appropriate to find the slope  $\frac{dz}{ds}$  at the axis of the grain boundary core. By differentiating Eq. (33), one gets

$$\left. \frac{dz}{ds} \right|_{s=0} = \frac{4 \tanh \frac{1}{4} z_0}{1 - (\tanh \frac{1}{4} z_0)^2} \quad (35)$$

and

$$\left. \frac{d\phi}{dx} \right|_{x=0} = \left. \frac{dz}{ds} \right|_{s=0} \frac{kT}{e} \kappa_+ , \quad (36)$$

so that

$$D' \delta = 4fa^2 v n' \delta \exp(-\Delta g_0 / kT) \left[ 1 + \frac{32\alpha kT}{e^2 (\kappa_+^{-1})^2} \times \left\{ \frac{\tanh(-\frac{e\phi_\infty}{4kT})}{1 - \left\{ \tanh(-\frac{e\phi_\infty}{4kT}) \right\}^2} \right\}^2 \right] . \quad (37)$$

For considering only the diffusion in the grain boundary, it is reasonable to limit the width of the space charge layer up to the grain boundary width. Therefore, in Eq. (37),  $\kappa_+^{-1}$  can be replaced by  $\delta/2$ . Thus

$$D' \delta = 4fa^2 v n' \delta \exp(-\Delta g_0 / kT) [1 + A] , \quad (38)$$

where now



$$A = \frac{32\alpha kT}{e^2 (\delta/2)^2} \left[ \frac{\tanh\left(-\frac{e\phi_\infty}{4kT}\right)}{1 - \left\{ \tanh\left(-\frac{e\phi_\infty}{4kT}\right) \right\}^2} \right]^2 \cdot \quad (39)$$

Eq. (38) can be used to explain the anomalous behavior of the  $\ln D'\delta$  vs  $1/T$  plots in Fig. 6. This equation clearly shows that two different factors contribute in evaluation of  $D'\delta$ : thermal activation contributes the term outside the square brackets multiplied by 1 while the electrical (polarization) effect contributes the term outside the square brackets multiplied by the factor A.

The numerical values of the factor A from the experimental plots (see Figs. 6 and 7) are observed to be 1.35 and 1.55 for the "pure" and the doped bicrystals, respectively. These values can be reproduced through Eq. (39) by substituting for the different parameters involved. Although the exact width of the grain boundary core is not known it can be approximated to be about  $6A^\circ$  as reported by Sun and Bauer<sup>39</sup> on the basis of their results on the mobility measurements of low and high-angle tilt grain boundaries in NaCl. For iodine  $\alpha$  is reported<sup>57</sup> to be  $9 \times 10^{-24} \text{ cm}^3$ . As region I is below the isoelectric temperature, it is reasonable to evaluate A for a temperature of  $400^\circ\text{K}$ , which is below the theoretical isoelectric temperature of "pure" NaCl

predicted by Kliewer and Koehler's theory. Using 0.19 eV and 0.20 eV for  $e\phi_{\infty}$  (these values are in the range reported by Kliewer and Koehler), calculated values of  $A$  are found to be 1.20 and 1.55, respectively, for "pure" NaCl. The difference in diffusion behavior of a hypothetical uncharged grain boundary and a real one can thus be accounted for by Eq. (38) thereby lending support to the model presented here. It is thus possible to reconstruct a schematic diagram (Fig. 7) of the  $\ln D'\delta$  vs  $1/T$  plots (Fig. 6) by means of Eq. (38) in the following manner.

In region I, the low temperature range, the high temperature equilibrium charged defects and the electrical field due to them are frozen in. Therefore, the dipole potential  $\phi$  present in this region is constant. The lower straight line in this diagram in region I corresponds to the thermal contribution to the grain boundary diffusivity. Due to the presence of the electrical field, the polarization of the iodine ions is increased which in turn increases the value of  $D'\delta$  by the factor  $A$ . When the temperature increases to a value  $T_{op}$ , then according to Kliewer and Koehler's theory, the dipole potential and the electrical field due to the dipole layer around the grain boundary become zero at this isoelectric temperature. As polarization of the ions is directly proportional to the electrical field present,<sup>58</sup> the

polarization of the iodine ions at  $T_{op}$  is minimal. Hence at  $T_{op}$ , factor A becomes zero and  $D'\delta$  shows a minimum - the observed  $D'\delta$  value at this temperature being due only to the thermal contribution to the grain boundary diffusivity. Region II corresponds to the transition range between region I and the minimum value of  $D'\delta$  at  $T_{op}$ .

As the temperature is increased above  $T_{op}$ , the dipole potential increases according to Kliever and Koehler's theory thereby giving increasing values of A with rising temperature.  $D'\delta$  is therefore effectively increased because of both the thermal activation and the electrical effect in region III. Contrary to the situation in region I, the dipole potential is not constant in region III but is increasing with increasing temperature. The slope of the  $\ln D'\delta$  vs  $1/T$  curve is thus observed to be different in region III than in region I because of a new equilibrium concentration of the charged defects and a corresponding dipole potential affecting the grain boundary diffusion in region III.

The rising trend in  $D'\delta$  is slowed in region IV as a result of two possible effects. First, according to Kliever and Koehler's theory, the dipole potential around the grain boundaries in NaCl tends to approach a saturation value at about 150°C above the isoelectric temperature. Region IV in the present experimental curves is about 40°C to 50°C from  $T_{op}$ . Since their theory is crude

in predicting an isoelectric temperature of 300°C for pure NaCl against their experimentally determined value of 460°C, it is plausible to believe that region IV in Figs. 6 and 7 falls in the temperature range where the dipole potential around the grain boundary begins to saturate. This saturation of the electrical field causes the polarization of iodine ions to level off and leads to a smaller slope of  $\ln D'\delta$  vs  $1/T$  curve in this region. Second, NaI and NaCl form a eutectic at about 570°C.<sup>59</sup> Thus the diffusion characteristics could possibly change because of proximity to the eutectic temperature in this region, thereby showing a behavior of the type observed in region IV. Present study had to be terminated at 570°C because of the experimental difficulties encountered due to the proximity to the melting point of NaI.

The mechanism of diffusion along the grain boundary can also be understood on the basis of the space charge concept. In the temperature range of region I, the grain boundaries are below their isoelectric temperature; thus they are negatively charged while the surrounding space charge regions are positive. Therefore, the grain boundary cores contain an excess of sodium vacancies or, equivalently, chlorine "interstitials" - and the surrounding space charge consists primarily of divalent cations. According to the space charge theory, below the

isoelectric temperature, the effective free energy of anion vacancy formation in the dipole layer is always greater than the actual free energy of anion vacancy formation in the bulk. If the free energy of motion of anion vacancies is assumed to be unchanged by their being in the dipole layer (a reasonable assumption for low defect concentrations at low temperatures), the activation energy for iodine diffusion by a single-vacancy mechanism in the space charge region should not be less than  $1.11 + 1.11 = 2.22$  eV (see Table IV). However, the experimentally determined activation energy of iodine diffusion in grain boundaries of "pure" NaCl is observed to be only 1.35 eV. Thus, the enhanced iodine diffusion in the grain boundaries of NaCl does not take place by a single-vacancy mechanism. A vacancy pair mechanism can similarly be ruled out for the observed iodine diffusion in NaCl grain boundaries due to the large activation energies required for vacancy pair diffusion (Table IV). Iodine ions have very high polarizability and therefore they would be deformable more easily.<sup>14</sup> Also, the observed value of activation energy for grain boundary diffusion is less than six tenths of the activation energy for single-vacancy diffusion in NaCl. The iodine ions should therefore move (wiggle through) in the highly distorted region of the grain boundary core by an "interstitial" type mechanism.

Thus, if the grain boundary diffusion is an intrinsic effect and if the grain boundaries conform to the predictions of the space charge theory, the observed enhanced iodine grain boundary diffusion seems to occur by the movement of "interstitial" iodine ions in the highly distorted grain boundary cores in the low temperature region while the polarization of the ions and the isoelectric temperature phenomenon lead to anomalous behavior of  $D'\delta$  at high temperatures. These conclusions are strengthened by observations of Laurant and Benard<sup>14</sup> that the large anions like iodine move more rapidly along the grain boundaries and that the iodine ions have the highest degree of polarization in the halogen series.

Since the shape of the  $\ln D'\delta$  vs  $1/T$  curve for doped bicrystals (Fig. 6) is very similar to the "pure" case and since four similar regions are observed in both cases, the mechanism of diffusion and the effect of polarization on  $D'\delta$  in the doped bicrystal can be explained in the manner analogous to the "pure" case. The major differences to be explained are that the values of  $D'\delta$  are smaller and that the minimum in  $D'\delta$  (which corresponds to the isoelectric temperature of the grain boundary) occurs at a lower temperature (493°C) in the doped bicrystal samples than in the "pure" samples.

The doped bicrystal contains a higher number of divalent impurity cations, both in the grain boundary and in the bulk. The mobility of the diffusing iodine ions in the grain boundary is lowered due to the very presence of these impurities and hence a larger activation energy is required for the movement of the diffusing iodine ions. The larger observed value of activation energy (1.93 eV), determined from the slope of the region I of the doped bicrystal diffusivity plot supports this expectation.

Kliwer and Koehler's theory predicts that the isoelectric temperature should increase with an increase of divalent cation impurities in NaCl. The present study indicates a slight decrease in the grain boundary isoelectric temperature with increase of calcium cations from 3 to  $142 \pm 5$  ppm. This observed reverse shift in the isoelectric temperature could result from a number of causes. Their theory assumed that in a sodium chloride crystal containing divalent impurities, all the impurities present were either in a free state or associated with a vacancy of the opposite charge. They did not consider higher complexes which might exist as impurity precipitates and aggregates of impurity-vacancy complexes. They also completely neglected any binding energies between point defects and dislocations and/or boundaries. Such an interaction of impurity and grain boundary could lead to some sort of "precipitate" at

the grain boundary. The presence of such complexes would serve to reduce the average concentration of divalent impurities in the material under investigation. The observed isoelectric temperature would therefore tend to be lower than the theoretically predicted values. Also, the formation of the precipitate would produce a new interface thereby changing the nature of the grain boundary itself. The argument about the existence of such complexes and precipitates is strengthened by the results of a number of investigators,<sup>11,60</sup> in diffusivity and conductivity measurements in sodium chloride crystals. An exact reason for the observed effect of the dopant on the isoelectric temperature can only be described after the detailed structure of high-angle grain boundaries becomes known.



## VII. CONCLUSIONS

Enhanced diffusion of  $^{131}\text{I}$  is observed along the tilt grain boundaries in "pure" and calcium chloride doped bicrystals of sodium chloride. The presence of the dopant lowers the grain boundary diffusivity. Thermal activation and electrical polarization effects, acting simultaneously on the diffusing ion, determine the magnitude of the grain boundary diffusivity in these ionic bicrystals. In the low temperature range of  $430^\circ\text{C}$  to  $490^\circ\text{C}$ , the diffusion of  $^{131}\text{I}$  along the grain boundaries is described by the relationship

$$D'\delta = (D'\delta)_0 \exp(-Q_b/kT), \quad (10)$$

where  $(D'\delta)_0$  has values of  $8.45 \times 10^{-5}$  and  $0.39 \text{ cm}^3/\text{sec}$  for the "pure" and the doped bicrystals, respectively.  $Q_b$  is observed to be 1.36 and 1.93 eV for the same two cases. In the high temperature range of  $490^\circ\text{C}$  to  $570^\circ\text{C}$ , grain boundary charge and ionic polarization cause distinct but similar diffusion anomalies in the grain boundary diffusivity plots of both the "pure" and doped bicrystals, depending upon the proximity of the measuring temperature to the isoelectric temperature. Grain boundary diffusion seems to occur by movement of ions in the grain boundary core region by an "interstitial" motion of iodine ions.

## BIBLIOGRAPHY

1. K. R. Riggs, Thesis, University of Missouri-Rolla (1970).
2. M. Chemla, Compt. Rend. 234, 2601 (1952); thesis, University of Paris (1956).
3. D. Mapother, N. Crooks, and R. Maurer, J. Chem. Phys. 18, 1231 (1950).
4. J. F. Laurant and J. Benard, J. Phys. Chem. Solids 3, 7 (1957).
5. N. Laurance, Phys. Rev. 120, 57 (1960).
6. L. G. Harrison, J. A. Morrison, and R. Rudham, Trans. Faraday Soc. 54, 106 (1958).
7. J. A. Morrison and R. Rudham, J. Phys. Chem. Solids 6, 402 (1958).
8. L. W. Barr, I. M. Hoodless, J. A. Morrison, and R. Rudham, Trans. Faraday Soc. 56, 697 (1960).
9. H. W. Etzel and R. J. Maurer, J. Chem. Phys. 18, 1003 (1950).
10. A. B. Lidiard, J. Phys. Chem. Solids 6, 298 (1958).
11. L. W. Barr, J. A. Morrison, and P. A. Schroeder, J. Appl. Phys. 36, 624 (1965).
12. R. G. Fuller, Phys. Rev. 142, 524 (1966).
13. J. C. Beaumont and J. Cabane, C. R. Acad. Sc. 252, 113 (1961).

14. J. F. Laurant and J. Benard, J. Phys. Chem. Solids 7, 218 (1958).
15. J. Cabane, J. Chem. Phys. 59, 1123 (1962).
16. I. M. Hoodless and S. J. Thomson, Phil. Mag. 46, 1131 (1959).
17. S. M. Klotsman, I. P. Polikarpova, A. N. Timofeev, and I. S. Trakhtenberg, Soviet Physics - Solid State 9, 1956 (1968).
18. R. Smoluchowski, in Imperfections in Nearly Perfect Crystals, W. Shockley-Editor (John Wiley, New York, 1952), p. 451.
19. M. L. Kronberg and F. H. Wilson, Trans. AIME 185, 501 (1949).
20. P. Beck and W. Hu, in Recrystallization, Grain Growth and Textures, Harold Margolin-Editor (ASM, Metals Park, Ohio, 1966), p. 393.
21. D. G. Brandon, B. Ralph, S. Ranganathan, and M. S. Wald, Acta Met. 12, 813 (1964).
22. J. Friedel, B. D. Culity, and C. Crussard, Acta Met. 1, 80 (1953).
23. M. Weins, H. Gleiter, and B. Chalmers, Scripta Met. 4, 235 (1970).
24. P. G. Shewmon, Diffusion in Solids (McGraw-Hill Book Co., Inc., New York, 1963).
25. R. Hoffman, Acta Met. 4, 98 (1956).
26. R. Smoluchowski, Phys. Rev. 87, 482 (1952).

27. G. H. Bishop, in Recrystallization, Grain Growth and Textures (ASM, Metals Park, Ohio, 1966), p. 200.
28. J. Frenkel, Kinetic Theory of Liquids (Oxford Univ. Press, New York, 1946), p. 36.
29. K. Lehovec, J. Chem. Phys. 21, 1123 (1953).
30. J. D. Eshelby, C. W. A. Newey, P. L. Pratt, and A. B. Lidiard, Phil. Mag. 3, 75 (1958).
31. J. S. Koehler, D. Langreth, and B. Von Turkovich, Phys. Rev. 128, 573 (1962).
32. K. L. Kliewer and J. S. Koehler, Phys. Rev. 140, A 1226 (1965).
33. R. B. Poepfel and J. M. Blakely, Surface Science 15, 507 (1969).
34. R. W. Davidge, Phys. Stat. Sol. 3, 1851 (1963).
35. R. W. Davidge, Phil. Mag. 8, 1369 (1963).
36. A. Hikita, C. Elbaum, B. Chick, and R. Truell, J. Appl. Phys. 34, 2154 (1963).
37. P. L. Pratt, Inst. Metals Monograph and Report Series 23, 99 (1957).
38. R. C. Sun and C. L. Bauer, Acta Met. 18, 639 (1970).
39. D. McLean, Grain Boundaries in Metals (Oxford Univ. Press, New York, 1957), p. 16.
40. K. Compain and Y. Haven, Trans. Faraday Soc. 52, 786 (1956).
41. H. R. Glyde, Rev. Mod. Phys. 39, 373 (1967).

42. H. S. Carslaw and J. C. Jaeger, Conduction of Heat in Solids (Oxford Univ. Press, New York, 1959), p. 50.
43. J. C. Fisher, J. Appl. Phys. 22, 74 (1951).
44. R. T. Whipple, Phil. Mag. 45, 1225 (1954).
45. T. Suzuka, Trans. Jap. Inst. Metals 2, 25 (1961).
46. V. G. Borisov and B. Ya. Lyubou, Fiz. Metallov. i Metallovedenie 1, 298 (1958).
47. Y. Y. Geguzin, G. M. Kovalev, and A. M. Ratner, Phys. Met. and Metallog. 10, 45 (1960).
48. H. S. Levine and C. J. MacCallum, J. Appl. Phys. 31, 595 (1960).
49. N. Fuschillo, M. L. Gimpl, and A. D. McMaster, J. Appl. Phys. 37, 2044 (1966).
50. Ernest M. Levin, Carl R. Robbins, and Howard F. McMurdie, Phase Diagrams for Ceramists (The American Cer. Soc., Inc., 1964) p. 384.
51. A. D. Leclaire, British J. Appl. Phys. 14, 351 (1963).
52. N. Laurance, Thesis, University of Illinois (1960).
53. G. A. Shirn, E. S. Wajda, and H. B. Huntington, Acta Met. 1, 513 (1953).
54. J. F. Laurant, Thesis, University of Paris (1958).
55. K. L. Kliewer and J. S. Koehler, Phys. Rev. 157, 685 (1967).

56. R. W. Dreyfus and A. S. Nowick, J. Appl. Phys. Suppl. 33, 473 (1962).
57. J. Norton Wilson and M. Curtis, J. Phys. Chem. 74, 187 (1970).
58. J. D. Jackson, Classical Electrodynamics (John Wiley, New York, 1962), p. 115.
59. Ernest M. Levin, Carl R. Robbins and Howard F. McMurdie, Phase Diagrams for Ceramists 1969 Supplement (The American Cer. Soc., Inc., 1969), p. 401.
60. R. W. Dreyfus and A. S. Nowick, Phys. Rev. 126, 1367 (1962).

## VITA

Kulwant Singh Sabharwal was born on January 11, 1944, in Peshawar, India (Now in Pakistan). He received his primary and secondary education in New Delhi, India and attended Indian Institute of Technology, Kharagpur, India, where he received the Bachelor of Technology Degree with honors in Metallurgical Engineering in January 1965. He worked as a metallurgist in Electrical Manufacturing Company, Aluminum Division, Calcutta, India from June, 1965 to August, 1967.

He was selected as a Rotary Foundation Fellow and was sponsored by Rotary International for the period September 1967 to May 1968 to do graduate study in the University of Missouri-Rolla, Rolla, Missouri. He received a Master of Science Degree in Metallurgical Engineering from that institution in October, 1969. The author has been a Graduate Research Assistant at the University of Missouri-Rolla, Rolla, Missouri from June 1968 to August 1972. He is the author of a previous publication: "Thermal Fatigue Testing of Die Casting Die Steels" (Society of Die Casting Engineers Trans., Paper No. 71, 1970).